remote sensing

MDPI

Article

Modelling Heat Balance of a Large Lake in Central Tibetan Plateau Incorporating Satellite Observations

Linan Guo [1], Hongxing Zheng [2], Yanhong Wu [3,4], Liping Zhu [1,*], Junbo Wang [1] and Jianting Ju [1]

[1] State Key Laboratory Tibetan Plateau Earth System, Environment and Resources (TPESER), Institute of Tibetan Plateau Research, Chinese Academy of Sciences, Beijing 100101, China; guoln@itpcas.ac.cn (L.G.)
[2] CSIRO Environment, Canberra, ACT 2601, Australia; hongxing.zheng@csiro.au
[3] International Research Center of Big Data for Sustainable Development Goals, Beijing 100094, China
[4] Key Laboratory of Digital Earth Science, Aerospace Information Research Institute, Chinese Academy of Sciences, Beijing 100094, China
* Correspondence: lpzhu@itpcas.ac.cn; Tel.: +86-10-84097093

Abstract: The thermodynamics of many lakes around the globe are shifting under a warming climate, affecting nutrients and oxygen transportation within the lake and altering lake biota. However, long-term variation in lake heat and water balance is not well known, particularly for regions like the Tibetan Plateau. This study investigates the long-term (1963–2019) variation in the heat balance of a large lake in the Tibetan Plateau (Nam Co) by combining the strengths of modeling and remote sensing. Remotely sensed lake surface water temperatures from the Moderate Resolution Imaging Spectroradiometer (MODIS) and Along Track Scanning Radiometer Reprocessing for Climate: Lake Surface Water Temperature and Ice Cover (ARC-Lake) are used to calibrate and validate a conceptual model (air2water) and a thermodynamic model (LAKE) for the studied lake, for which in situ observation is limited. The results demonstrate that remotely sensed lake surface water temperature can serve as a valuable surrogate for in situ observations, facilitating effective calibration and validation of lake models. Compared with the MODIS-based lake surface water temperature (LSWT) for the period 2000–2019, the correlation coefficient and root mean square error (RMSE) of the LAKE model are 0.8 and 4.2 °C, respectively, while those of the air2water model are 0.9 and 2.66 °C, respectively. Based on modeling, we found that the water temperature of Nam Co increased significantly ($p < 0.05$) during the period of 1963–2019, corresponding to a warming climate. The rate of water temperature increase is highest at the surface layer (0.41 °C/10a). This warming trend is more noticeable in June and November. From 1963 to 2019, net radiation flux increased at a rate of 0.5 W/m^2/10a. The increase in net radiation is primarily responsible for the warming of the lake water, while its impact on changes in lake evaporation is comparatively minor. The approaches developed in this study demonstrate the flexibility of incorporating remote sensing observations into modeling. The results on long-term changes in heat balance could be valuable for a systematic understanding of lake warming in response to a changing climate in the Tibetan Plateau.

Keywords: lake energy balance; lake thermal process; lake temperature; Tibetan Plateau

Citation: Guo, L.; Zheng, H.; Wu, Y.; Zhu, L.; Wang, J.; Ju, J. Modelling Heat Balance of a Large Lake in Central Tibetan Plateau Incorporating Satellite Observations. *Remote Sens.* **2023**, *15*, 3982. https://doi.org/10.3390/rs15163982

Academic Editor: Natascha Oppelt

Received: 16 June 2023
Revised: 30 July 2023
Accepted: 8 August 2023
Published: 11 August 2023

1. Introduction

Lakes are vital reservoirs of liquid water on Earth, with lower albedo and roughness but a higher heat capacity than their surrounding terrestrial environment. Lakes are also essential sources of moisture for the lower atmosphere [1,2] and sentinels of climate change [3,4]. It has been reported that many lakes around the globe are warming at rates higher than their ambient air temperature [5,6]. This warming trend reflects changes in the thermodynamics of lakes and the corresponding heat balance, resulting in intensifying lake stratification in summer [7,8] and shorter ice duration for lakes in the cryosphere [9]. These changes have shown impacts on nutrients and oxygen transportation between the

surface and deep water of lakes, altering the vertical distribution and composition of lake biota [10].

Shifts in lake thermodynamics and heat balance in response to a changing climate have attracted increasing research efforts to improve our knowledge of the interactions between lakes and the climate [11–14] and the physical and ecological consequences of a warming lake [15,16]. The research includes studies based on ground observation, remote sensing data, and modeling. Ground-based research is largely limited to a local scale due to its high costs and data availability [17]. More research is now based on remotely sensed data (like surface water temperature) to investigate the changes in lake thermodynamics at a broader scale [18,19]. Remote sensing provides various observations not only to monitor the dynamics of the hydrothermal characteristics of lakes but also to calibrate or validate lake models at different temporal and spatial scales.

On top of the observation-based research, lake modeling plays an important role in quantitively describing the thermodynamics and processes of lake heat balance, as well as their responses to a changing environment [20]. Various lake models have been developed to simulate the thermodynamics of lakes around the world. The models could be of different conceptualization and complexity depending on the research goals and available resources, including 1-D/2-D/3-D process-based models [21–25] or simplified physically-based models [26]. The 1-D LAKE model is one of the models that presents a compromise between the explicit resolution of key physical processes and computational efficiency [25,27,28]. This model allows for high-temporal resolution input data and high computational efficiency to effectively reproduce the thermodynamics of lakes. On the other hand, the air2water model is a simplified, physically based model with minimal requirements for model input [29].

The Tibetan Plateau (TP), known as the "water tower" of Asia, is a cold region with thousands of lakes. The thermodynamics and heat balance of the lakes, however, are rarely known, mainly due to the high cost of ground-based observations. More research efforts on the thermodynamics of the lakes in the TP are now based on the increasing availability of space-based observations. For example, Wan et al. (2017) and Liu et al. (2019) have used AVHRR and MODIS to produce lake surface water temperature datasets across the TP [18,30]. More recently, Guo et al. (2022) and Wu et al. (2022) have combined remote sensing with modeling to reconstruct lake surface temperature [31] and lake ice phenology [32] for more than 130 lakes across the TP. Both ground-based and space-based observations have shown that thermal conditions, together with other physical characteristics (like water levels and surface water extents) of lakes in the Tibetan Plateau, are changing substantially [33–36]. It has been noticed that lakes in the TP are experiencing a faster warming rate than that of global land surface air temperature over the period of 1979–2012 [37,38], which has caused considerable impacts on water and heat balance within the region and beyond. However, more research is needed to further the thermodynamics of lakes and their response to a changing climate through process-based modeling [39]. The modeling could contribute to quantifying the impacts of climate change on components of the heat balance of a lake and predicting their potential change under future climate scenarios [40,41].

The objective of this study is to detect the long-term variation in the thermodynamics and heat balance of the Nam Co, which is the second-largest lake in the Tibetan Autonomous Region. Two lake models (air2water and LAKE 2.3) are used in this study to reconstruct the long-term time series of lake temperature and components of heat balance for the period 1963–2019. Remotely sensed data (MODIS and ARC-Lake) are used to calibrate and validate the lake models. The approaches developed in this study show the flexibility of incorporating remote sensing data into modeling while improving the modeling capability for understanding the connections between lake thermodynamics and climate.

2. Materials and Methods

2.1. Study Area

The Nam Co Lake (Figure 1) is located at 90°16′–91°03′E, 30°30′–30°55′N, with a mean elevation of 4718 m a.s.l. and an area of 2026 km^2. The maximum depth is over 100 m, and the mean depth of Nam Co is about 40 m. It occupies a closed basin, and there is no surface outflow. Precipitation and glacier melt water are the main water supplies for Nam Co, accounting for 23–28% and 7–22%, respectively. Observations suggest that the lake is a dimictic lake characterized by thermal stratification from late June to early November [42] and generally ice-covered from January or February to April or May [32]. The lake is located in the monsoon-influenced transition zone between semi-humid and semi-arid areas. The annual mean air temperature of Nam Co is approximately 0 °C, and precipitation is about 450 mm/a [43,44]. In the warm–rainy (May to September) season, its precipitation constitutes 91% of the total annual precipitation [43,44]. The mean annual wind speed is 4 m/s, with the maximum monthly mean speed of 6.1 m/s occurring in January (You et al., 2007). The annual evaporation from the lake surface is still uncertain, although some studies have reported estimates such as 635 mm [45] or 832 ± 69 mm from Lazhu [46].

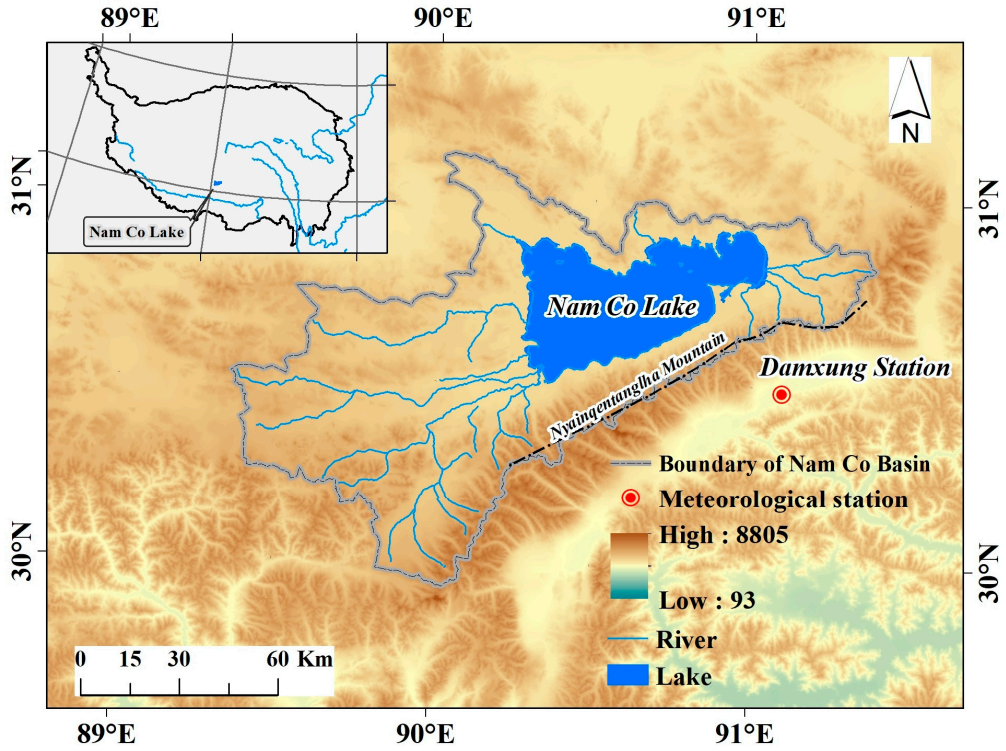

Figure 1. Location of the study area.

2.2. Data

The air2water model requires only air temperature as an input, while the required meteorological inputs for the LAKE 2.3 model include air temperature, specific humidity, air pressure, wind speed, shortwave radiation, longwave radiation, and precipitation. The meteorological data used for modeling in this study are from the Damxung station (91°06′E, 30°29′N) for the period of 1963–2019, obtained from the CMA (China Meteorological Administration). The Damxung station is the nearest available meteorological station to the Nam Co. The air temperature above the lake is estimated based on the station observations with a lapse rate of 0.65 °C/100 m [47], while the air pressure is corrected by the Barometric formula. Based on relative humidity, saturation vapor pressure (calculated by the Bolton formula), and air temperature, the specific humidity is obtained. The longwave and

shortwave radiations are calculated from sunshine duration, latitude, air temperature, and vapor pressure.

The daily land surface temperature data from the Moderate Resolution Imaging Spectroradiometer (MODIS) for the period of 2000–2019 are retrieved to calibrate the air2water model and validate the simulation results from both the air2water and LAKE models. The product MOD11A1 has a spatial resolution of 1 km. The mean lake surface water temperature (LSWT) is calculated by removing pixels from the lake boundary. The bias of MODIS-derived LSWT versus in situ observation for lakes in the TP is −1.74 °C [48] and −1.4 °C [49]. For model validation, the ARC-Lake dataset (version 3) is also used, which includes ATSR-2/AATSR-based daily lake surface temperatures for the period 1995–2012 for 1628 target water bodies distributed globally. Herein, the ARC-Lake daytime and nighttime LSWTs are averaged to present the daily mean LSWT. The ARC-Lake LSWT product is only for seasons with open water, while the LSWT for the frozen season is considered to have no data. This product is widely used in LSWT calibration or validation globally [50], with mean absolute error ranges from −0.34 to −0.09 °C (day) and −0.18 to +0.06 °C (night) [51].

3. Method

3.1. LAKE Model and Configuration

LAKE 2.3 is a 1-D model of thermodynamic, hydrodynamic, and biogeochemical processes in a lake [25]. The model uses the generic form of the Reynolds-averaged advection–diffusion equation to describe horizontal velocity components, temperature, turbulent kinetic energy (TKE), TKE dissipation, and concentration of multiple biogeochemical species such as gases (O_2, CO_2, and CH_4) and organic carbon variables. The lake thermodynamics include a heat diffusion formulation where heat conductance is a sum of molecular and turbulent coefficients estimated by the $k-\varepsilon$ model [25]. The lake thermodynamic processes include heat and moisture transfer in the water body, snow cover, soil, and heat balance at the lake surface. For more details about the model, refer to the references cited [25,52,53].

Most parameters of the LAKE model have clear physical meanings and are free from calibration. In setting up the LAKE model for Nam Co, lake properties, including longitude, latitude, area, and depth, are required. In this study, the depth of Nam Co is set to 80 m, and the lake is vertically represented by 160 layers (0.5 m for each layer). The boundary condition is assumed to be the Neuman boundary condition for free convection. The model is highly sensitive to the extinction coefficient of lake water (0.07–0.17/m), which is the only model parameter considered for calibration in this study. The LAKE model needs a relatively long warming-up period, which is set at 20 years herein.

3.2. Air2Water Model and Modification

The air2water model proposed by Piccolroaz et al. (2013) is a hybrid model with a strong physical basis that simplifies the thermodynamic equations to minimize the input requirement while preserving the robustness of deterministic models [29]. The model is an effective tool in reconstructing historical LSWT [50,54,55] and in investigating LSWT responses to climate change for lakes with different morphological characteristics around the world [56,57]. The original air2water model has simplified the lake heat balance by introducing eight calibratable parameters, a_{1-8}, with air temperature as the only required input, which can be expressed as

$$\frac{dT_w}{dt} = \frac{1}{\delta}\left\{a_1 + a_2 T_a - a_3 T_w + a_5 cos\left[2\pi\left(\frac{t}{t_y} - a_6\right)\right]\right\}, \tag{1}$$

$$\delta = \begin{cases} exp\left(-\frac{T_w - T_h}{a_4}\right), & for\ T_w \geq T_h \\ exp\left(-\frac{T_h - T_w}{a_7}\right) + exp\left(-\frac{T_w}{a_8}\right), & for\ T_w \leq T_h \end{cases}. \tag{2}$$

where T_a is the air temperature and t_y is the number of days in a year. $\delta = D/D_r$ is the normalized well-mixed depth, where D is the depth of the well-mixed surface layer (the epilimnion thickness), D_r is the maximum thickness, and T_h is the deep water temperature, with the default value being 4 °C.

To overcome the limitation of air2water in the ice season simulation, we assume that when the lake is completely covered by ice, the heat exchange between air and water is blocked, and the surface energy balance is expressed as Equation (3) [31]. The lake surface temperature, T_L, is finally expressed as Equation (4):

$$\frac{dT_i}{dt} = a_9 + a_{10}T_a - a_{11}T_w + a_{12}cos\left[2\pi\left(\frac{t}{t_y} - a_{13}\right)\right], \tag{3}$$

$$T_L = \begin{cases} T_w, & for\ \ T_L \geq a_{15} \\ T_i, & for\ \ T_L \leq a_{14} \\ (1 - K_{ice})T_w + K_{ice}T_i, & for\ a_{15} > T_L > a_{14} \end{cases}. \tag{4}$$

where T_i is the ice surface temperature, and a_{9-13} has similar physical significance to $a_{1,2,3,5,6}$. $K_{ice} = \sqrt{(a_{15} - T_L)/(a_{15} - a_{14})}$ is the proportion of ice on the surface of the lake.

3.3. Model Calibration and Validation

For model calibration, we compare the modeled LSWT against the remotely sensed LSWT, utilizing daily land surface temperature data from MODIS for the period of 2000–2019. The objective function for model calibration is the Nash-Sutcliffe efficiency coefficient (NSE), which is expressed as [58]:

$$NSE = 1 - \frac{\sum_{t=1}^{T}(Q_o - Q_m)^2}{\sum_{t=1}^{T}\left(Q_o - \overline{Q_o}\right)^2} \tag{5}$$

where Q_m is the simulated lake surface water temperature, Q_o is the LSWT from MODIS, and $\overline{Q_o}$ is the mean value of the LSWT from MODIS. For the modified air2water model, there are 14 parameters that need to be calibrated, which are implemented automatically by using the particle swarm optimizer (PSO). For the LAKE model, since only the extension coefficient needs to be calibrated within a narrow range, manual trial-and-error calibration is then applied.

For model validation, lake surface water temperature datasets from both MODIS and ARC-Lake are used. With the consideration of outliers in the MODIS LSWT dataset, LSWT lower than −15 °C is excluded for model calibration and validation. Meanwhile, the ARC-Lake dataset is only used for validating model performance for seasons with LSWT above 0 °C. In addition, in situ water temperature observations of Nam Co for the period from November 2011 to June 2014 were obtained from the National Tibetan Plateau Data Center to evaluate the performance of the LAKE model at different depths (for model validation). The in situ observations were made by VEMCO Minilog-II-T at 3, 6, 16, 21, and 26 m depths in the lake. The criteria used for model evaluation are coefficient of determination (R^2) and root mean squared error (RMSE), which are expressed as:

$$R^2 = \frac{\sum_{i=1}^{n}\left(Q_{pre} - \overline{Q_m}\right)^2}{\sum_{i=1}^{n}\left(Q_m - \overline{Q_m}\right)^2} \tag{6}$$

$$RMSE = \sqrt{\frac{1}{n}\sum_{i=1}^{n}(Q_m - Q_o)^2} \tag{7}$$

where Q_{pre} is the predicted temperature of linear regression, $\overline{Q_m}$ is the mean value of the modeled temperature, and Q_o is the temperature from in situ or satellite observations.

4. Results

4.1. Model Performance

Figure 2 shows the performances of air2water and LAKE and their comparison against the satellite-based observations from MODIS (2000–2019) and ARC-Lake (1995–2012), respectively. The results show the mean monthly LSWT and long-term mean daily LSWT for each calendar date. The calibration periods of the air2water and LAKE models are 2000–2012 and 2000–2019, respectively. The calibrated extinction coefficient of the LAKE model is 0.1, which is consistent with the experiment based on the Flake model, CoLM-Lake model, and WRF-Lake model in Huang et al. (2019) [59].

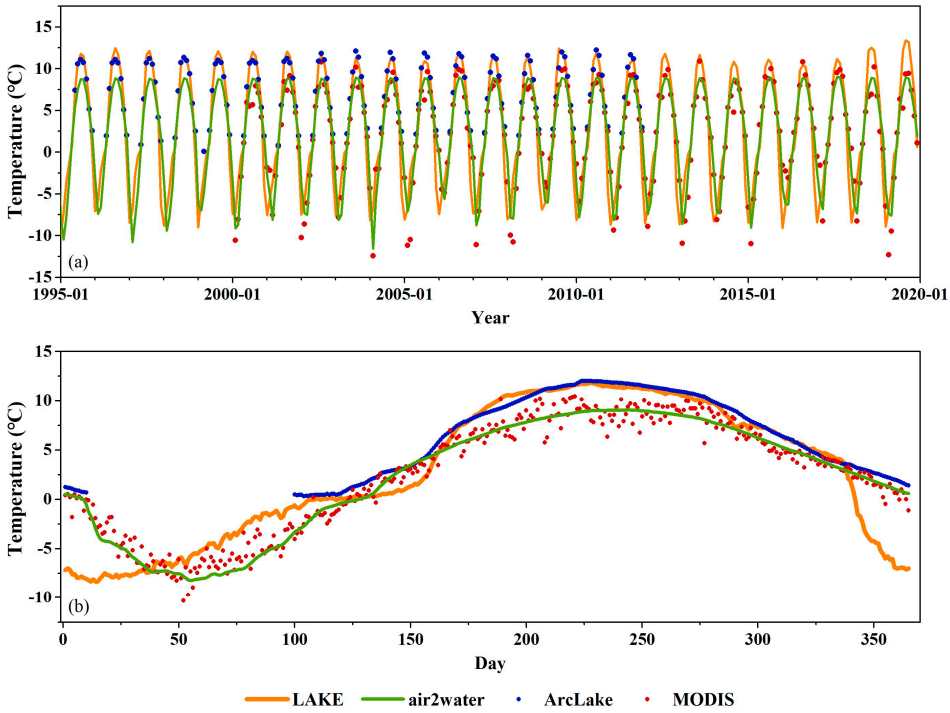

Figure 2. Comparison between simulated LSWT and remote sensing data (**a**) monthly and (**b**) long-term mean daily.

The air2water model overall is in good agreement with the satellite-based observations. For the calibration period (2000–2012), the correlation coefficients between air2water and MODIS are 0.895 on the daily scale and 0.977 on the monthly scale. The corresponding RMSE compared to MODIS is 2.66 °C on the daily scale and 1.23 °C on the monthly scale. For the validation period (2013–2019), the correlation coefficients between air2water and MODIS are 0.90 on the daily scale and 0.967 on the monthly scale, with corresponding RMSEs of 1.87 °C on the daily scale and 1.47 °C on the monthly scale. The correlation coefficients between air2water and ARC-Lake are 0.967 on the daily scale and 0.979 on the monthly scale, with RMSEs of 1.99 °C on the daily scale and 1.92 °C on the monthly scale. It is found that air2water underestimates the LSWT observed by ARC-Lake for summer (JJA) but overestimates the LSWT observed by MODIS for winter (DJF). The simulated LSWTs of spring and autumn are in good agreement with the remote-sensing water temperature. This is mainly because the simulated lake water temperature from air2water is not completely equivalent to the lake surface water temperature observed by satellites. The simulated temperature from air2water represents the surface water temperature instead of the skin temperature (~10–20μm deep) from the satellite.

The Surface water temperature simulated by the LAKE model shows strong agreement with that from satellite-based observations. The model performs consistently during 1995–2019, with correlation coefficients (R) against LSWT of MODIS and ARC-Lake of 0.80 and 0.92 on the daily scale and 0.88 and 0.93 on the monthly scale, respectively, for the

entire time period. The RMSE of LAKE's LSWT is 4.19 °C against MODIS LST and 3.19 °C against ARC-Lake LSWT. It is worth noting that the LAKE model is highly comparable with ARC-Lake's observation for the surface water temperature in summer (JJA) but is higher than the observations from MODIS.

We further compare the simulated lake water temperature from the LAKE model against in situ observations at the depths of 3 m, 6 m, 16 m, 21 m, 26 m, and 31 m in the Nam Co Lake for the period from 31 October 2012 to 1 July 2014, with the results shown in Figure 3. The LAKE model, with our calibrated model settings, could reproduce well the overall features of the observed temperature profiles for this period. In particular, for water temperatures at 3 m and 6 m, the simulated temperature from the LAKE model is in good agreement with that from in situ observations, with NSEs of 0.9 and 0.84 and RMSEs of 0.75 °C and 1.07 °C, respectively. For water temperature at a depth of 16 m, the model performs well for the cooling period (October–January) but underestimates water temperature for the warming period (February–September). The model tends to underestimate water temperature at deeper layers (e.g., 21 m, 26 m, and 31 m) of the lake. The model tends to underestimate the depth of the mixing layer, resulting in an underestimate of water temperature at deeper layers. Compared to in situ observation, the model performs well during the ice-free season (June to November) but presents a relatively thinner mixed layer from September to October and a shallower thermocline in the ice season (December to February).

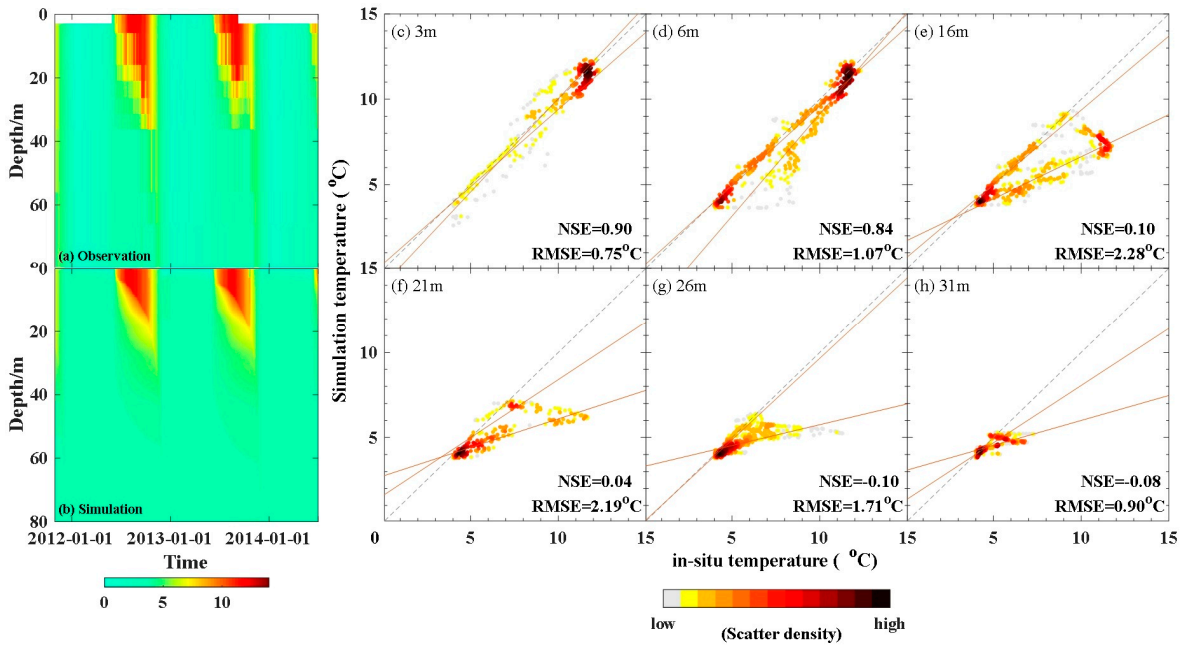

Figure 3. Comparison between (**b**) simulated and (**a**) in-situ temperature profiles, (**c**–**h**) is the scatter plot at the depths of 3 m, 6 m, 16 m, 21 m, 26 m, and 31 m.

Overall, the error of the simulation results of conceptual models (air2water) and physical models compared to remote sensing and in situ observation is acceptable for long-term research. It indicates that it is feasible to use remote sensing data as calibration data for the model in the absence of long-term in situ lake surface temperature data. Since the LAKE model is physically based and presents richer thermodynamic characteristics of the lake, we use the simulation results from LAKE to investigate the seasonal and inter-annual variation in lake temperature and thermodynamics in the subsequent sections.

4.2. Seasonal Variation in Lake Temperature and Thermodynamics

Figure 4 shows the seasonal dynamics of lake water temperature profiles from the LAKE model. As a dimictic lake, the water temperature of layers below 40 m (hypolimnion)

in Nam Co is about 4 °C. The lake water is warming up and is completely mixed around mid-June (Figure 4b). Summer stratification occurs in late June in response to the enhanced heating from the lake surface. The depth of the mixing layer was about 20 m in late June. The temperature of the mixing layer increases to 11 °C in mid-August, and the temperature gradient (from 0 to 40 m depth of the lake) gradually reaches the annual maximum at 0.2 °C/m (Figure 4c). From July to October, the lake holds its summer stratification. However, since early September, the temperature of the surface layer has decreased gradually because of weaker radiation and turbulent heat loss. From October to November, the temperature of the upper water layer decreases from 8 °C to 4 °C, and the vertical temperature gradient continues to reduce until the water column is completely mixed again from top to bottom (Figure 4d). From December to late May of the next year, the water column of the lake maintains an inverse thermal stratification, i.e., winter stratification (Figure 4e).

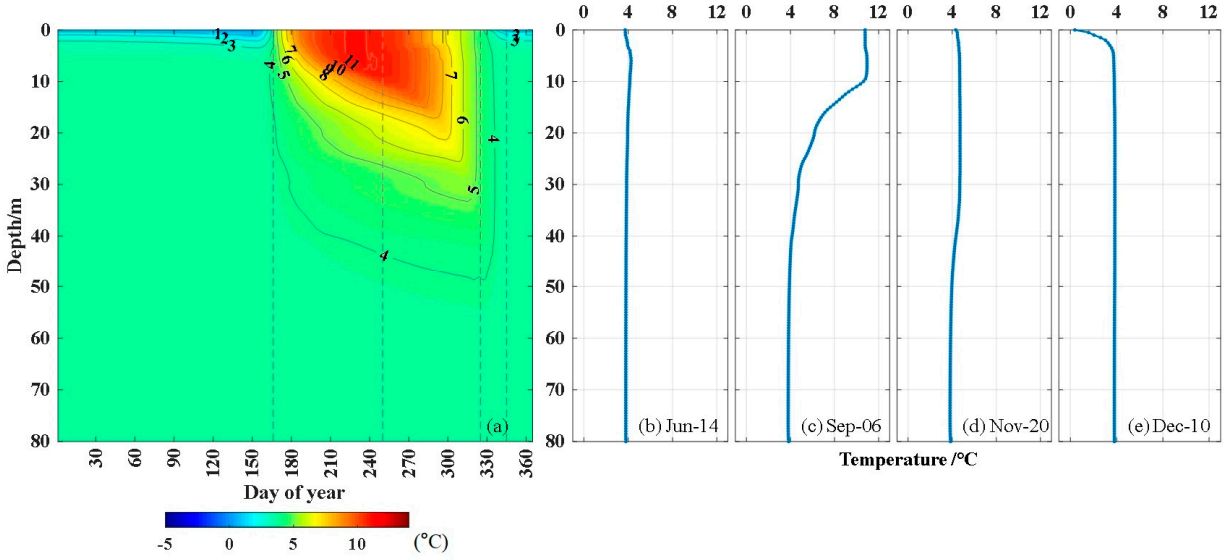

Figure 4. Seasonal variation in lake water temperature. (**a**) Temperature profiles for each calendar date averaged over the period of 1963–2019; (**b**–**e**) representative temperature profiles for the summer, autumn, winter, and spring seasons, respectively.

The seasonal variation in lake thermodynamics based on simulations from the LAKE model is shown in Figure 5, which is the climatological mean from 1963 to 2019. The net radiation Rn reaches its lowest in December, peaks in June, and is mainly affected by Rs_{net}. In Nam Co, sensible heat flux (H) ranges from -20 to 32 W/m^2. The sensible heat flux is negative in May and June, indicating that the lake water temperature is lower than the air temperature for that period. The latent heat flux (LE) shows two peaks in a year (early April and mid-October). It is worth noting that the seasonal pattern of LE is different from that of Rn, indicating that lake evaporation depends more on other climate variables (like wind speed). The incoming radiation largely contributes to warming up the water in the lake, as represented by the change in heat storage (S). The results suggest that Nam Co has a high heat storage capacity, which can remarkably influence the phase of the seasonal variation in the lake surface turbulent fluxes [60–62]. The lake's surface temperature responds more quickly to changes in energy. With the increase in net radiation Rn, $T_{surface}$ has started to rise since mid-January and reaches its peak in August. However, due to the buffering effect of its high heat storage capacity, the temperature of the water column, T_{water}, had increased gradually since May, when S became positive, but decreased starting in mid-September, when S became negative.

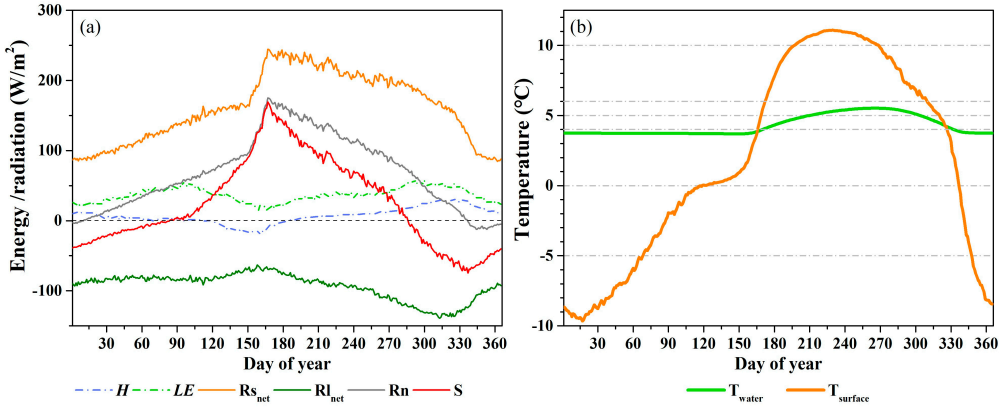

Figure 5. Seasonal variation in lake thermodynamics: (**a**) H, LE, Rs_{net}, Rl_{net}, Rn and S represent sensible heat flux, potential heat flux, net solar radiation, net longwave radiation, net radiation, and gain or loss of heat, respectively, with $Rn = Rs_{net} + Rl_{net}$ and $S = Rn - H - LE$; (**b**) water temperature of lake surface ($T_{surface}$) and water column (T_{water}).

4.3. Long-Term Changes in Lake Temperature and Heat Balance

For the period of 1963–2009, the water temperature based on the LAKE model in Nam Co is found to be increasing significantly ($p < 0.05$) together with a significant ($p < 0.05$) decrease in the depth of the thermocline (Figure 6). The warming rate of the lake surface water temperature (LSWT) is 0.41 °C/10a, which is higher than the air temperature (0.38 °C/10a). The mean temperature of the water column is warming at a rate of 0.04 °C/10a. The thermocline depth, where the maximum value of the temperature gradient occurs [63], is declining at a rate of 1.56 m/10a, accompanied by a warming trend. This declination trend is in agreement with previous research in Nam Co [64] and other lakes in the temperate zone [65,66].

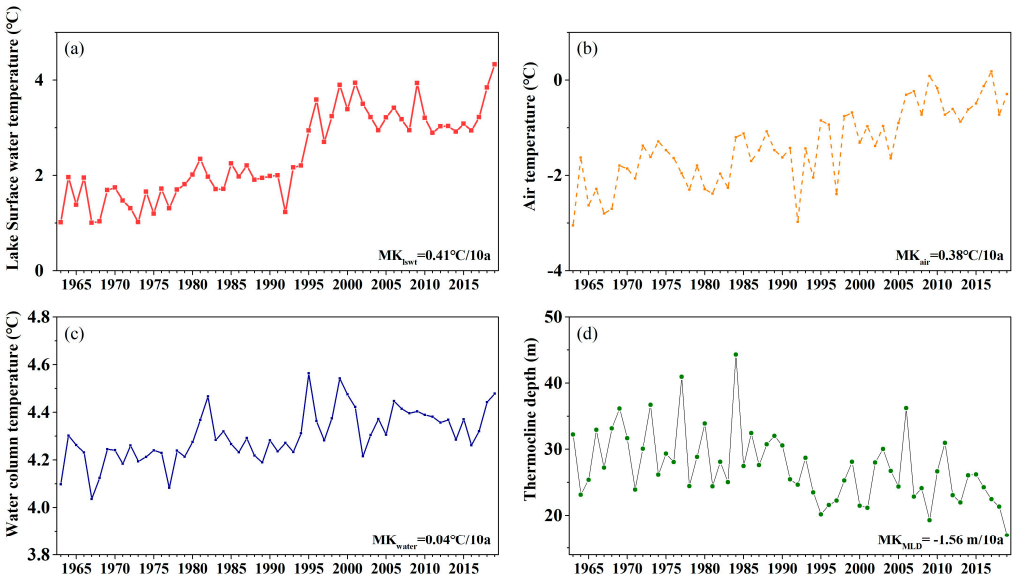

Figure 6. Long-term change in (**a**) lake surface temperature, (**b**) air temperature, (**c**) water column mean temperature, and (**d**) thermocline depth of the non-freezing season (June to November).

Figure 7 shows the long-term change in each heat balance element during the past 57 years. Rs_{net} increases at a rate of 1.4 W/m^2 per decade. Rl_{net} (upward) increases at a rate of 0.7 W/m^2 per decade. Rn increases significantly ($p < 0.05$) at a rate of 0.5 W/m^2/10a. Sensible heat flux (H), determined by the temperature difference between the surface water and the overlying atmosphere, does not change much. Meanwhile, the latent heat flux

(*LE*) decreases slightly at a rate of 0.2 W/m^2/10a but is not significant. The energy balance residual (*S*) increases at a rate of 0.7 W/m^2 per decade. The increasing loss of heat explains the corresponding increase in water temperature. It should be noted that *S* is considered an approximate measure of the net heat gained by the lake. However, it implicitly includes other heat flux elements, such as heat transfer to the bottom sediments, net heat exchange resulting from inflow–outflow balances, and heat gained from precipitation over the lake [67].

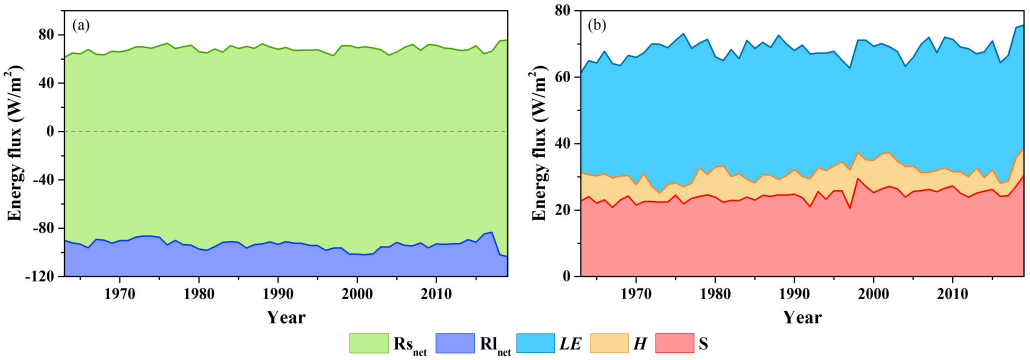

Figure 7. Inter-annual variation in energy flux from 1963 to 2019 (**a**) latent heat flux (*LE*), sensible heat flux (*H*), and energy balance residual (*S*); (**b**) net shortwave radiation (Rs_{net}) and net longwave radiation (Rl_{net}).

Figure 8 further shows the long-term trend in water temperature at different layers (Figure 8a) and the trend in each heat balance element (Figure 8b) for each month, detected using the Mann–Kendall (MK) approach [68,69]. The water temperature at the surface layer increases at the highest rate in December (0.92 °C/10a), followed by that in June (0.62 °C/10a). The seasonal differences in the long-term trend in surface water temperature are largely consistent with those in air temperature. The warming trend of water weakens with depth. For water below 20 m, the increasing trend is not statistically significant ($p < 0.05$) except for November (0.1 °C/10a).

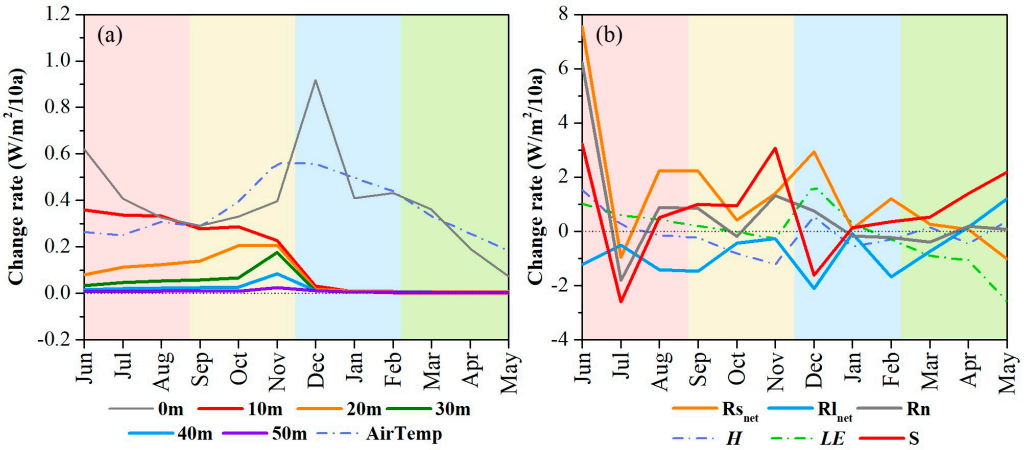

Figure 8. Inter-annual Mann–Kendall trend of monthly (**a**) lake temperatures at different depths and (**b**) energy flux during 1963–2019: net radiation (*Rn*), net shortwave radiation (Rs_{net}), net longwave radiation (Rl_{net}), sensible heat flux (*H*), latent heat flux (*LE*), and energy balance residual (*S*).

During the past 57 years, Rs_{net} in June has been found to increase at the highest rate (7.6 W/m^2/10a), making a major contribution to the higher heat gain *S* (8 W/m^2/10a) and hence warmer lake water in that season. With the increase in surface water temperature, sensible heat flux (*H*) increases most significantly ($p < 0.05$) in June (1.5 W/m^2/10a). The seasonal pattern of trend in latent heat flux (*LE*) is similar to that of sensible heat flux.

However, a higher change rate in *LE* is found in December (1.7 $W/m^2/10a$), followed by June (1.0 $W/m^2/10a$). The results suggest that the increasing lake evaporation could be attributed not only to the increase in net radiation (Rn) but also to increases in other climate factors (e.g., wind speed and vapor pressure deficit under a warming climate).

5. Discussion

5.1. Roles of Remote Sensing Data in Models

Numerical models play an important role in investigating the dynamics of lake water and heat balances. In particular, the physically based thermodynamic models can be used to reproduce the long-term variation and change in each heat balance element and to quantify their responses to climate change and other environmental changes (e.g., land use and land cover change). However, the models require reliable observations for model calibration and validation prior to their utilization. Traditionally, observations for model calibration or validation are mainly in situ measurements [57]. However, in situ observations are not easily available or sufficient for model calibration or validation in regions like the Tibetan Plateau, where in situ measurements can incur high costs.

Satellite-based observations have shown great potential for providing continuous records of lake thermodynamics over large spatial extents and have developed rapidly in recent decades with increasingly higher temporal and spatial resolutions [70,71]. Remote sensing offers distinct advantages in simultaneously measuring the thermodynamic status of a lake at a broader scale, surpassing the limitations of traditional in situ point-scale observations. Therefore, satellite-based observations are increasingly used to provide various inputs, parameters, or outputs information to drive, calibrate, or validate numerical models [72]. For example, in our previous study, we used the MODIS LST dataset to calibrate/validate the air2water model for 160 lakes across the Tibetan Plateau. We reconstructed the long-term daily water temperature of the lakes [31]. Without satellite data, it is nearly impossible to evaluate the simulation accuracy for every lake. Layden et al. (2016) used LSWT data derived from Along Track Scanning Radiometers (ATSRs) to calibrate the Flake model [26] and provide the LSWT for 244 large lakes [72].

However, calibrating or validating a thermodynamic model, such as the LAKE model, primarily using remotely sensed lake surface water temperature (LSWT), does not guarantee accurate simulation of every aspect of lake thermodynamics. Therefore, besides lake surface temperature, other remote sensing information (such as lake ice cover, remotely sensed evaporation, etc.) would be valuable for more robust model calibration and validation, which could be further explored in the future. It is also noticed that the numbers of model parameters are assigned constant values, which is a compromise due to observation insufficiency and model complexity. For instance, for the LAKE model used in this study, the light extinction coefficient is the only parameter calibrated, while the other parameters are accepted as default. This could lead to considerable uncertainty in the simulation of other lakes if their properties are substantially different. Some parameters of lake models can be obtained from satellite observation, such as albedo, emissivity, lake area, water level, etc. Incorporating more satellite-based observations could therefore be expected to further improve model performance. However, the quality of the remotely sensed data should be carefully checked, and the consistency among the remotely sensed data should also be assessed prior to their use for modeling.

It is worth noting that information obtained from satellites captures solely the instantaneous status of the lake (e.g., surface temperature, ice cover, etc.) when the sensors pass over it. Therefore, satellite-based observations may not match well with the time intervals of lake models. For instance, the time interval of the lake models used in this study is daily, but the remotely sensed surface water temperature was acquired at 10:30 local time. The temporal mismatch can pose challenges for model calibration and validation. To address this, the remotely sensed data used for modeling may require preprocessing, which includes cleaning (such as removing outliers), interpolation, or smoothing techniques. These

procedures could be as important as model calibration procedures and worth more notice in the future.

5.2. The Warming Trend of Nam Co

In this study, the error of the simulation results of conceptual models (air2water) and physical models compared to remote sensing and in situ observation is acceptable for long-term research. Thus, in regions lacking in situ lake temperature data, such as the Tibetan Plateau, it is feasible for remote sensing data to serve as a surrogate in lake thermodynamic simulations. Overall, the LAKE model performs well in Nam Co compared with observations from remote sensing or in situ measurements. It is also comparable with the conceptual lake model (i.e., air2water) in modeling lake water temperature.

According to the simulation results of the LAKE model, the lake temperature of Nam Co showed a significant warming trend from 1963 to 2019. It is generally believed that changes in water temperature are caused by global warming [5,55] and climate oscillations [3,66]. This study also shows the agreement between changes in lake temperature and air temperature (Figure 6a,b). The lake temperature is warming at a rate of 0.04 °C/10a based on the LAKE model. Besides air temperature, input energy is also an important driver for lake warming, including the increase in net solar radiation (Rs_{net}) at 1.4 W/m^2 per decade (Figure 7). Thus, the increasing gain (0.7 W/m^2/10a) of heat explains the corresponding increase in water temperature. The decline in the thermocline depth at a rate of 1.56 m/10a (1963–2019) is in agreement with the previous research in Nam Co at 1.69 m/10a (1979–2012) [64]. The warming of lakes increased their thermal stability and resistance to mixing, which influences the efficiency of the downward vertical transport of warm metalimnetic water into the hypolimnion, which especially happens in hot summers.

6. Conclusions

This study investigates the long-term variation in the heat balance of Nam Co by combining the strengths of modeling and remote sensing. Remotely sensed lake surface water temperatures from MODIS and ARC-Lake are used to calibrate or validate a conceptual model (air2water) and a thermodynamic model (LAKE) for the studied lake, where in situ observations are limited. The research has demonstrated that remotely sensed lake surface water temperature can serve as a valuable surrogate for in situ observations, facilitating effective calibration and validation of lake models. Compared to MODIS-based LSWT for the period of 2000–2019, the correlation coefficient and RMSE of the LAKE model are 0.8 and 4.2 °C, respectively, while those of the air2water model are 0.9 and 2.66 °C, respectively.

Based on the simulations using the LAKE model, it is found that the water temperature of Nam Co has experienced a significant increase during the period of 1963–2019, corresponding to a warming climate. The rate of the water temperature increase is the highest at the surface layer (0.41 °C/10a) but becomes negligible at the bottom of the lake. The increasing rate of water temperature averaged over the profile is 0.04 °C/10a. This warming trend is more noticeable in June and November. Concurrently, the thermocline depth in Nam Co is found to be declining at a rate of 1.56 m/10a. Most of the net radiation entering Nam Co is stored in the water from April to August and is then released starting in mid-September. From 1963 to 2019, net radiation flux increased at a rate of 0.5 W/m^2/10a and showed the highest increase rate in June (around 6 W/m^2/10a). The increase in net radiation is primarily responsible for the warming of the lake water, while its impact on changes in lake evaporation is comparatively minor.

Integrating remote sensing into process-based modeling can enhance our understanding of the thermodynamic processes occurring in lakes at larger spatial and temporal scales after uncertainty is assessed. This integration can enable us to assess the ecological implications resulting from changes in lake heat balance.

Author Contributions: Conceptualization, H.Z. and Y.W.; methodology, L.G. and H.Z.; software, L.G. and H.Z.; validation, Y.W.; investigation, J.W. and J.J.; writing—original draft preparation, L.G.; writing—review and editing, H.Z., Y.W. and L.Z.; visualization, L.G.; supervision, L.Z.; funding acquisition, L.G. All authors have read and agreed to the published version of the manuscript.

Funding: This research was funded by the Second Tibetan Plateau Scientific Expedition and Research Program under Grant 2019QZKK0202 and the Youth Fund of the National Natural Science Foundation of China under Grant 42201145.

Data Availability Statement: Not applicable.

Acknowledgments: We gratefully acknowledge the Climate Data Center, the National Meteorological Information Center, and the China Meteorological Administration for providing the long-term meteorological data for the Damxung station.

Conflicts of Interest: The authors declare no conflict of interest.

References

1. Biermann, T.; Babel, W.; Ma, W.Q.; Chen, X.L.; Thiem, E.; Ma, Y.M.; Foken, T. Turbulent flux observations and modelling over a shallow lake and a wet grassland in the Nam Co basin, Tibetan Plateau. *Theor. Appl. Climatol.* **2014**, *116*, 301–316. [CrossRef]
2. Xiao, C.L.; Lofgren, B.M.; Wang, J.; Chu, P.Y. Improving the lake scheme within a coupled WRF-lake model in the Laurentian Great Lakes. *J. Adv. Model. Earth Syst.* **2016**, *8*, 1969–1985. [CrossRef]
3. Adrian, R.; O'Reilly, C.M.; Zagarese, H.; Baines, S.B.; Hessen, D.O.; Keller, W.; Livingstone, D.M.; Sommaruga, R.; Straile, D.; Van Donk, E.; et al. Lakes as sentinels of climate change. *Limnol. Oceanogr.* **2009**, *54*, 2283–2297. [CrossRef] [PubMed]
4. Schindler, D.W. Lakes as sentinels and integrators for the effects of climate change on watersheds, airsheds, and landscapes. *Limnol. Oceanogr.* **2009**, *54*, 2349–2358. [CrossRef]
5. O'Reilly, C.M.; Sharma, S.; Gray, D.K.; Hampton, S.E.; Read, J.S.; Rowley, R.J.; Schneider, P.; Lenters, J.D.; McIntyre, P.B.; Kraemer, B.M.; et al. Rapid and highly variable warming of lake surface waters around the globe. *Geophys. Res. Lett.* **2015**, *42*, 10773–10781. [CrossRef]
6. Austin, J.A.; Colman, S.M. Lake Superior summer water temperatures are increasing more rapidly than regional air temperatures: A positive ice-albedo feedback. *Geophys. Res. Lett.* **2007**, *34*, L06604. [CrossRef]
7. Danis, P.A.; von Grafenstein, U.; Masson-Delmotte, V.; Planton, S.; Gerdeaux, D.; Moisselin, J.M. Vulnerability of two European lakes in response to future climatic changes. *Geophys. Res. Lett.* **2004**, *31*, L21507. [CrossRef]
8. Sahoo, G.B.; Forrest, A.L.; Schladow, S.G.; Reuter, J.E.; Coats, R.; Dettinger, M. Climate change impacts on lake thermal dynamics and ecosystem vulnerabilities. *Limnol. Oceanogr.* **2016**, *61*, 496–507. [CrossRef]
9. Butcher, J.B.; Nover, D.; Johnson, T.E.; Clark, C.M. Sensitivity of lake thermal and mixing dynamics to climate change. *Clim. Change* **2015**, *129*, 295–305. [CrossRef]
10. Woolway, R.I.; Merchant, C.J. Worldwide alteration of lake mixing regimes in response to climate change. *Nat. Geosci.* **2019**, *12*, 271. [CrossRef]
11. Gu, H.P.; Jin, J.M.; Wu, Y.H.; Ek, M.B.; Subin, Z.M. Calibration and validation of lake surface temperature simulations with the coupled WRF-lake model. *Clim. Change* **2015**, *129*, 471–483. [CrossRef]
12. Li, Z.G.; Lyu, S.H.; Ao, Y.H.; Wen, L.J.; Zhao, L.; Wang, S.Y. Long-term energy flux and radiation balance observations over Lake Ngoring, Tibetan Plateau. *Atmos. Res.* **2015**, *155*, 13–25. [CrossRef]
13. Eerola, K.; Rontu, L.; Kourzeneva, E.; Pour, H.K.; Duguay, C. Impact of partly ice-free Lake Ladoga on temperature and cloudiness in an anticyclonic winter situation–a case study using a limited area model. *Tellus A Dyn. Meteorol. Oceanogr.* **2014**, *66*, 23929. [CrossRef]
14. Ma, X.G.; Yang, K.; La, Z.; Lu, H.; Jiang, Y.Z.; Zhou, X.; Yao, X.N.; Li, X. Importance of Parameterizing Lake Surface and Internal Thermal Processes in WRF for Simulating Freeze Onset of an Alpine Deep Lake. *J. Geophys. Res.-Atmos.* **2022**, *127*, e2022JD036759. [CrossRef]
15. O'Reilly, C.M.; Alin, S.R.; Plisnier, P.D.; Cohen, A.S.; McKee, B.A. Climate change decreases aquatic ecosystem productivity of Lake Tanganyika, Africa. *Nature* **2003**, *424*, 766–768. [CrossRef]
16. O'Beirne, M.D.; Werne, J.P.; Hecky, R.E.; Johnson, T.C.; Katsev, S.; Reavie, E.D. Anthropogenic climate change has altered primary productivity in Lake Superior. *Nat. Commun.* **2017**, *8*, 15713. [CrossRef]
17. Sharma, S.; Gray, D.K.; Read, J.S.; O'Reilly, C.M.; Schneider, P.; Qudrat, A.; Gries, C.; Stefanoff, S.; Hampton, S.E.; Hook, S.; et al. A global database of lake surface temperatures collected by in situ and satellite methods from 1985–2009. *Sci. Data* **2015**, *2*, 150008. [CrossRef] [PubMed]
18. Wan, W.; Li, H.; Xie, H.; Hong, Y.; Long, D.; Zhao, L.; Han, Z.; Cui, Y.; Liu, B.; Wang, C. A comprehensive data set of lake surface water temperature over the Tibetan Plateau derived from MODIS LST products 2001–2015. *Sci. Data* **2017**, *4*, 170095. [CrossRef] [PubMed]
19. Guo, L.; Wu, Y.; Zheng, H.; Zhang, B.; Li, J.; Zhang, F.; Shen, Q. Uncertainty and Variation of Remotely Sensed Lake Ice Phenology across the Tibetan Plateau. *Remote Sens.* **2018**, *10*, 1534. [CrossRef]

20. Janssen, A.B.G.; Arhonditsis, G.B.; Beusen, A.; Bolding, K.; Bruce, L.; Bruggeman, J.; Couture, R.M.; Downing, A.S.; Elliott, J.A.; Frassl, M.A.; et al. Exploring, exploiting and evolving diversity of aquatic ecosystem models: A community perspective. *Aquat. Ecol.* **2015**, *49*, 513–548. [CrossRef]
21. Goudsmit, G.H.; Burchard, H.; Peeters, F.; Wuest, A. Application of k-epsilon turbulence models to enclosed basins: The role of internal seiches. *J. Geophys. Res.-Ocean.* **2002**, *107*, 23-1–23-13. [CrossRef]
22. Kirillin, G.; Wen, L.J.; Shatwell, T. Seasonal thermal regime and climatic trends in lakes of the Tibetan highlands. *Hydrol. Earth Syst. Sci.* **2017**, *21*, 1895–1909. [CrossRef]
23. Launiainen, J.; Cheng, B. Modelling of ice thermodynamics in natural water bodies. *Cold Reg. Sci. Technol.* **1998**, *27*, 153–178. [CrossRef]
24. Peeters, F.; Livingstone, D.M.; Goudsmit, G.H.; Kipfer, R.; Forster, R. Modeling 50 years of historical temperature profiles in a large central European lake. *Limnol. Oceanogr.* **2002**, *47*, 186–197. [CrossRef]
25. Stepanenko, V.; Mammarella, I.; Ojala, A.; Miettinen, H.; Lykosov, V.; Vesala, T. LAKE 2.0: A model for temperature, methane, carbon dioxide and oxygen dynamics in lakes. *Geosci. Model Dev.* **2016**, *9*, 1977–2006. [CrossRef]
26. Mironov, D.V. *Parameterization of Lakes in Numerical Weather Prediction: Description of a Lake Model*; Technical Report no. 11; ARPA Piemonte: Offenbach, Germany, 2008.
27. Stepanenko, V.M.; Machul'skaya, E.E.; Glagolev, M.V.; Lykossov, V.N. Numerical Modeling of Methane Emissions from Lakes in the Permafrost Zone. *Izv. Atmos. Ocean. Phys.* **2011**, *47*, 252–264. [CrossRef]
28. Iakunin, M.; Stepanenko, V.; Salgado, R.; Potes, M.; Penha, A.; Novais, M.H.; Rodrigues, G. Numerical study of the seasonal thermal and gas regimes of the largest artificial reservoir in western Europe using the LAKE 2.0 model. *Geosci. Model Dev.* **2020**, *13*, 3475–3488. [CrossRef]
29. Piccolroaz, S.; Toffolon, M.; Majone, B. A simple lumped model to convert air temperature into surface water temperature in lakes. *Hydrol. Earth Syst. Sci.* **2013**, *17*, 3323–3338. [CrossRef]
30. Liu, B.J.; Wan, W.; Xie, H.J.; Li, H.; Zhu, S.Y.; Zhang, G.Q.; Wen, L.J.; Hong, Y. A long-term dataset of lake surface water temperature over the Tibetan Plateau derived from AVHRR 1981–2015. *Sci. Data* **2019**, *6*, 48. [CrossRef]
31. Guo, L.A.; Zheng, H.X.; Wu, Y.H.; Fan, L.X.; Wen, M.X.; Li, J.S.; Zhang, F.F.; Zhu, L.P.; Zhang, B. An integrated dataset of daily lake surface water temperature over the Tibetan Plateau. *Earth Syst. Sci. Data* **2022**, *14*, 3411–3422. [CrossRef]
32. Wu, Y.; Guo, L.; Zhang, B.; Zheng, H.; Fan, L.; Chi, H.; Li, J.; Wang, S. Ice phenology dataset reconstructed from remote sensing and modelling for lakes over the Tibetan Plateau. *Sci. Data* **2022**, *9*, 743. [CrossRef] [PubMed]
33. Lu, S.L.; Jia, L.; Zhang, L.; Wei, Y.P.; Baig, M.H.A.; Zhai, Z.K.; Meng, J.H.; Li, X.S.; Zhang, G.F. Lake water surface mapping in the Tibetan Plateau using the MODIS MOD09Q1 product. *Remote Sens. Lett.* **2017**, *8*, 224–233. [CrossRef]
34. Phan, V.H.; Lindenbergh, R.; Menenti, M. ICESat derived elevation changes of Tibetan lakes between 2003 and 2009. *Int. J. Appl. Earth Obs. Geoinf.* **2012**, *17*, 12–22. [CrossRef]
35. Wu, Y.; Zhu, L. The response of lake-glacier variations to climate change in Nam Co Catchment, central Tibetan Plateau, during 1970–2000. *J. Geogr. Sci.* **2008**, *18*, 177–189. [CrossRef]
36. Zhu, L.P.; Xie, M.P.; Wu, Y.H. Quantitative analysis of lake area variations and the influence factors from 1971 to 2004 in the Nam Co basin of the Tibetan Plateau. *Chin. Sci. Bull.* **2010**, *55*, 1294–1303. [CrossRef]
37. Hartmann, D.L.; Tank, A.M.K.; Rusticucci, M.; Alexander, L.V.; Brönnimann, S.; Charabi, Y.A.R.; Dentener, F.J.; Dlugokencky, E.J.; Easterling, D.R.; Kaplan, A. Observations: Atmosphere and surface. In *Climate Change 2013 the Physical Science Basis: Working Group I Contribution to the Fifth Assessment Report of the Intergovernmental Panel on Climate Change*; Cambridge University Press: Cambridge, UK, 2013; pp. 159–254.
38. Kuang, X.X.; Jiao, J.J. Review on climate change on the Tibetan Plateau during the last half century. *J. Geophys. Res.-Atmos.* **2016**, *121*, 3979–4007. [CrossRef]
39. Guo, Y.H.; Zhang, Y.S.; Ma, N.; Song, H.T.; Gao, H.F. Quantifying Surface Energy Fluxes and Evaporation over a Significant Expanding Endorheic Lake in the Central Tibetan Plateau. *J. Meteorol. Soc. Jpn.* **2016**, *94*, 453–465. [CrossRef]
40. Wang, B.; Ma, Y.; Chen, X.; Ma, W.; Su, Z.; Menenti, M. Observation and simulation of lake-air heat and water transfer processes in a high-altitude shallow lake on the Tibetan Plateau. *J. Geophys. Res.-Atmos.* **2015**, *120*, 12327–12344. [CrossRef]
41. Wen, L.J.; Lyu, S.H.; Kirillin, G.; Li, Z.G.; Zhao, L. Air-lake boundary layer and performance of a simple lake parameterization scheme over the Tibetan highlands. *Tellus Ser. A-Dyn. Meteorol. Oceanogr.* **2016**, *68*, 31091. [CrossRef]
42. Wang, J.; Huang, L.; Ju, J.; Daut, G.; Ma, Q.; Zhu, L.; Haberzettl, T.; Baade, J.; Mäusbacher, R.; Hamilton, A. Seasonal stratification of a deep, high-altitude, dimictic lake: Nam Co, Tibetan Plateau. *J. Hydrol.* **2020**, *584*, 124668. [CrossRef]
43. Guan, Z.H.; Chen, C.Y.; Ou, Y.X.; Fan, Y.Q.; Zhang, Y.S.; Chen, Z.M.; Bao, S.H.; Zu, Y.T.; He, X.W.; Zhang, M.T. *Rivers and Lakes in Tibet*; Science Press: Beijing, China, 1984.
44. Ma, Y.-Z.; Yi, C.-L.; Wu, J.-Z.; Jin, Y. Lake surface expansion of Nam Co during 1970-2009: Evidence of satellite remote sensing and cause analysis. *J. Glaciol. Geocryol.* **2012**, *34*, 81–88.
45. Ma, N.; Szilagyi, J.; Niu, G.-Y.; Zhang, Y.; Zhang, T.; Wang, B.; Wu, Y. Evaporation variability of Nam Co Lake in the Tibetan Plateau and its role in recent rapid lake expansion. *J. Hydrol.* **2016**, *537*, 27–35. [CrossRef]
46. Lazhu; Yang, K.; Wang, J.; Lei, Y.; Chen, Y.; Zhu, L.; Ding, B.; Qin, J. Quantifying evaporation and its decadal change for Lake Nam Co, central Tibetan Plateau. *J. Geophys. Res.-Atmos.* **2016**, *121*, 7578–7591. [CrossRef]
47. Hu, Q.; Jiang, D.; Fan, G. Evaluation of CMIP5 models over the Qinghai-Tibetan Plateau. *Chin. J. Atmos. Sci.* **2014**, *38*, 924–938.

48. Song, K.; Wang, M.; Du, J.; Yuan, Y.; Ma, J.; Wang, M.; Mu, G. Spatiotemporal Variations of Lake Surface Temperature across the Tibetan Plateau Using MODIS LST Product. *Remote Sens.* **2016**, *8*, 854. [CrossRef]
49. Zhang, G.Q.; Yao, T.D.; Xie, H.J.; Qin, J.; Ye, Q.H.; Dai, Y.F.; Guo, R.F. Estimating surface temperature changes of lakes in the Tibetan Plateau using MODIS LST data. *J. Geophys. Res.-Atmos.* **2014**, *119*, 8552–8567. [CrossRef]
50. Piccolroaz, S.; Woolway, R.I.; Merchant, C.J. Global reconstruction of twentieth century lake surface water temperature reveals different warming trends depending on the climatic zone. *Clim. Change* **2020**, *160*, 427–442. [CrossRef]
51. Layden, A.; Merchant, C.; MacCallum, S. Global climatology of surface water temperatures of large lakes by remote sensing. *Int. J. Climatol.* **2015**, *35*, 4464–4479. [CrossRef]
52. Stepanenko, V.; Lykossov, V. Numerical modeling of heat and moisture transfer processes in a system lake-soil. *Russ. Meteorol. Hydrol.* **2005**, *3*, 95–104.
53. Stepanenko, V.M.; Valerio, G.; Pilotti, M. Horizontal Pressure Gradient Parameterization for One-Dimensional Lake Models. *J. Adv. Model. Earth Syst.* **2020**, *12*, e2019MS001906. [CrossRef]
54. Czernecki, B.; Ptak, M. The impact of global warming on lake surface water temperature in Poland—The application of empirical-statistical downscaling, 1971–2100. *J. Limnol.* **2018**, *77*, 330–348. [CrossRef]
55. Schmid, M.; Koster, O. Excess warming of a Central European lake driven by solar brightening. *Water Resour. Res.* **2016**, *52*, 8103–8116. [CrossRef]
56. Piccolroaz, S.; Toffolon, M.; Majone, B. The role of stratification on lakes' thermal response: The case of Lake Superior. *Water Resour. Res.* **2015**, *51*, 7878–7894. [CrossRef]
57. Prats, J.; Danis, P.A. An epilimnion and hypolimnion temperature model based on air temperature and lake characteristics. *Knowl. Manag. Aquat. Ecosyst.* **2019**, *24*, 8. [CrossRef]
58. Nash, J.E.; Sutcliffe, J.V. River flow forecasting through conceptual models part I—A discussion of principles—ScienceDirect. *J. Hydrol.* **1970**, *10*, 282–290. [CrossRef]
59. Huang, A.N.; Lazhu; Wang, J.B.; Dai, Y.J.; Yang, K.; Wei, N.; Wen, L.J.; Wu, Y.; Zhu, X.Y.; Zhang, X.D.; et al. Evaluating and Improving the Performance of Three 1-D Lake Models in a Large Deep Lake of the Central Tibetan Plateau. *J. Geophys. Res.-Atmos.* **2019**, *124*, 3143–3167. [CrossRef] [PubMed]
60. Blanken, P.D.; Spence, C.; Hedstrorn, N.; Lenters, J.D. Evaporation from Lake Superior: 1. Physical controls and processes. *J. Great Lakes Res.* **2011**, *37*, 707–716. [CrossRef]
61. Schertzer, W.M.; Rouse, W.R.; Blanken, P.D.; Walker, A.E. Over-lake meteorology and estimated bulk heat exchange of Great Slave Lake in 1998 and 1999. *J. Hydrometeorol.* **2003**, *4*, 649–659. [CrossRef]
62. Haginoya, S.; Fujii, H.; Kuwagata, T.; Xu, J.Q.; Ishigooka, Y.; Kang, S.C.; Zhang, Y.J. Air-Lake Interaction Features Found in Heat and Water Exchanges over Nam Co on the Tibetan Plateau. *Sola* **2009**, *5*, 172–175. [CrossRef]
63. Hambright, K.D.; Gophen, M.; Serruya, S. Influence of long-term climatic changes on the stratification of a subtropical, warm monomictic lake. *Limnol. Oceanogr.* **1994**, *39*, 1233–1242. [CrossRef]
64. Huang, L.; Wang, J.B.; Zhu, L.P.; Ju, J.T.; Daut, G. The Warming of Large Lakes on the Tibetan Plateau: Evidence from a Lake Model Simulation of Nam Co, China, During 1979–2012. *J. Geophys. Res.-Atmos.* **2017**, *122*, 13095–13107. [CrossRef]
65. Arvola, L.; George, G.; Livingstone, D.M.; Jrvinen, M.; Weyhenmeyer, G.A. The Impact of the Changing Climate on the Thermal Characteristics of Lakes. In *The Impact of Climate Change on European Lakes*; Springer: Dordrecht, The Netherlands, 2009.
66. Shimoda, Y.; Azim, M.E.; Perhar, G.; Ramin, M.; Kenney, M.A.; Sadraddini, S.; Gudimov, A.; Arhonditsis, G.B. Our current understanding of lake ecosystem response to climate change: What have we really learned from the north temperate deep lakes? *J. Great Lakes Res.* **2011**, *37*, 173–193. [CrossRef]
67. Wang, B.B.; Ma, Y.M.; Ma, W.Q.; Su, Z.B. Physical controls on half-hourly, daily, and monthly turbulent flux and energy budget over a high-altitude small lake on the Tibetan Plateau. *J. Geophys. Res.-Atmos.* **2017**, *122*, 2289–2303. [CrossRef]
68. Mann, H.B. Nonparametric Tests Against Trend. *Econometrica* **1945**, *13*, 245–259. [CrossRef]
69. Kendall, M.G. *Rank Correlation Methods*, 2nd ed.; Hafner Publishing Co.: London, Britain, 1955.
70. Prats, J.; Reynaud, N.; Rebiere, D.; Peroux, T.; Tormos, T.; Danis, P.A. LakeSST: Lake Skin Surface Temperature in French inland water bodies for 1999-2016 from Landsat archives. *Earth Syst. Sci. Data* **2018**, *10*, 727–743. [CrossRef]
71. Schneider, P.; Hook, S.J. Space observations of inland water bodies show rapid surface warming since 1985. *Geophys. Res. Lett.* **2010**, *37*, L22405. [CrossRef]
72. Layden, A.; MacCallum, S.N.; Merchant, C.J. Determining lake surface water temperatures worldwide using a tuned one-dimensional lake model (FLake, v1). *Geosci. Model Dev.* **2016**, *9*, 2167–2189. [CrossRef]